Journal of Inorganic Biochemistry 102 (2008) 1719–1730

Contents lists available at ScienceDirect

Journal of Inorganic Biochemistry

journal homepage: www.elsevier.com/locate/jinorgbio

Synthesis, crystal structures, cytotoxicity and qualitative structure–activity relationship (QSAR) of *cis*-*bis*{5-[(*E*)-2-(aryl)-1-diazenyl]quinolinolato} di-*n*-butyltin(IV) complexes, $^{n}Bu_2Sn(L)_2$

Tushar S. Basu Baul [a,*], Archana Mizar [a], Asit K. Chandra [a], Xueqing Song [b], George Eng [b], Robert Jirásko [c], Michal Holčapek [c], Dick de Vos [d], Anthony Linden [e,*]

[a] Department of Chemistry, North-Eastern Hill University, NEHU Permanent Campus, Umshing, Shillong, Meghalaya 793 022, India
[b] Department of Chemistry and Physics, University of the District of Columbia, Washington DC 20008, USA
[c] University of Pardubice, Department of Analytical Chemistry, Studentská 95, Pardubice, Czech Republic
[d] Pharmachemie BV, P.O. Box 552, 2003 RN Haarlem, The Netherlands
[e] Institute of Organic Chemistry, University of Zurich, Winterthurerstrasse 190, CH-8057 Zurich, Switzerland

ARTICLE INFO

Article history:
Received 14 February 2008
Received in revised form 20 April 2008
Accepted 29 April 2008
Available online 13 May 2008

Keywords:
5-[(*E*)-2-(aryl)-1-diazenyl]quinolin-8-ol
Di-*n*-butyltin(IV) complexes
NMR
ESI–MS
^{119m}Sn Mössbauer
Cytotoxicity
Crystal structures

ABSTRACT

A series of *cis*-*bis*{5-[(*E*)-2-(aryl)-1-diazenyl]quinolinolato}di-*n*-butyltin(IV) complexes has been synthesized and characterized by ^{1}H-, ^{13}C-, ^{119}Sn NMR, ESI–MS (electrospray ionization mass spectrometry), IR and ^{119m}Sn Mössbauer spectroscopic techniques in combination with elemental analyses. The structures of four di-*n*-butyltin(IV) complexes, *viz.*, $^{n}Bu_2Sn(L^3)_2$ (**3**), $^{n}Bu_2Sn(L^4)_2$ (**4**), $^{n}Bu_2Sn(L^5)_2$ (**5**) and $^{n}Bu_2Sn(L^7)_2 \cdot 0.5C_6H_6$ (**7**) (LH = 5-[(*E*)-2-(aryl)-1-diazenyl)quinolin-8-ol) were determined by single crystal X-ray diffraction. In general, the complexes were found to adopt a distorted *cis*-octahedral arrangement around the tin atom. These complexes retain their solid-state structure in non-coordinating solvent as evidenced by ^{119}Sn and ^{13}C NMR spectroscopic results. The *in vitro* cytotoxicity of di-*n*-butyltin(IV) complexes (**3–8**) is reported against seven well characterized human tumour cell lines. The basicity of the two quinolinolato donor N and O atoms of the ligands are discussed in relation to the cytotoxicity data.

1. Introduction

The chemical, biological and pharmaceutical properties of diorganotin(IV) complexes have been studied extensively. The structure–antitumour activity relationships of di- and triorganotin(IV) quinolin-8-olate(s) and antitumour activity of organotin(IV) derivatives are also well documented [1,2]. The organotin(IV) quinolin-8-olate(s) were also subjected to NMR spectroscopic techniques, such as ^{119}Sn, ^{15}N, ^{13}C and ^{1}H NMR, as well as solid state ^{119}Sn CP MAS, in order to have comprehensive state of the art understanding of the subject [3,4]. The derivation of the coordination number of the tin atom and the type of distortion of the coordination polyhedron of diorganotin(IV) complexes is not completely reliable when based only on ^{119}Sn NMR chemical shift data. Consequently, the structures of a few organotin(IV) quinolin-8-olates have been investigated by X-ray crystallography. The diorganotin(IV) *bis*(quinolin-8-olate) group of compounds has received the most attention and the crystal structures of R_2SnL_2 complexes, where R = Me [5], *p*-ClPh and *p*-MePh [6], ^{n}Bu and Cl [7], ^{n}Bu [8], ^{t}Bu [8] and Ph [9], showed molecules with a highly distorted octahedral coordination of the tin atom by bidentate quinolin-8-olate groups and essentially *cis*-R groups. In addition, structural information on two other types, *viz.*, R_2SnLX (e.g. R = $EtCO_2Me$; X = Cl) [10] and $RSnL_3$ (R = *p*-ClPh) [11] are also available. Recently, we have also reported the structures of six diorganotin(IV) complexes of the type R_2SnL_2 (R = Ph or Bz; L = 5-[(*E*)-2-(aryl)-1-diazenyl]-quinolin-8-olate) [12,13] and these complexes also conform to the same distorted *cis*-octahedral geometry described for diorganotin(IV) *bis*(quinolin-8-olate). On the other hand, there has been some disagreement concerning the solid state structure of Ph_3SnL, with both four- [14] and five-co-ordinate [15] structures having been assigned on the basis of ^{119}Sn Mössbauer from the magnitude of the quadrupole splitting. Finally, it was concluded that Ph_3SnL (L = quinolin-8-olate) is five coordinate with a trigonal bipyramidal coordination geometry where two phenyl groups and a nitrogen atom are in equatorial positions while a phenyl group and an oxygen atom from the quinolin-8-olate ligand take up the axial

* Corresponding authors. Tel.: +91 364 2722626; fax: +91 364 2721000 (T.S. Basu Baul), tel.: +41 44 635 4228; fax: +41 44 635 6812 (A. Linden).
E-mail addresses: basubaul@nehu.ac.in, basubaul@hotmail.com (T.S. Basu Baul), alinden@oci.uzh.ch (A. Linden).

0162-0134/$ - see front matter © 2008 Elsevier Inc. All rights reserved.
doi:10.1016/j.jinorgbio.2008.05.001

positions in *facial*-R_3 geometry [15]. To resolve these issues, we have recently reported the crystal structures of four Ph_3SnL compounds (L = 5-[(*E*)-2-(aryl)-1-diazenyl]quinolin-8-olate where the aryl group is an R′-substituted phenyl ring e.g. R′ = H; 2′-CH_3; 4′-OCH_3; 4′-OC_2H_5) which represent the first examples of structurally characterized triphenyltin(IV) compounds containing quinolin-8-olate ligand [16]. The results of the X-ray studies indicated that the Ph_3SnL complex (R′ = 2′-CH_3) is distorted trigonal–bipyramidal, with a phenyl C atom and the quinolin-8-olate N atom in axial positions, while three other benzene solvated compounds (R′ = H; 4′-OCH_3; 4′-OC_2H_5) have a distorted square pyramidal coordination geometry with one of the phenyl C atoms in the apical position.

Thus, the recent work on the synthesis and characterization of organotin(IV) complexes of compositions R_2SnL_2 (Bz, Ph) and Ph_3SnL (L = 5-[(*E*)-2-(aryl)-1-diazenyl)quinolin-8-olates) is greatly motivated by the substantial interest in their molecular structures and cytotoxic potentials [12,13,16].

In addition, organotin(IV) compounds are a widely studied class of metal-based antitumour drugs and their intensive investigation has led to the discovery of compounds with excellent in vitro antitumour activity, but, in many cases, disappointingly low in vivo potency or high in vivo toxicity [17–19]. It is well established that organotin(IV) compounds are very important in cancer chemotherapy because of their apoptotic inducing character [20,21]. The design of improved organotin(IV) antitumour agents occupy a significant place in cancer chemotherapy as revealed from their remarkable therapeutic potential reflected from the recent research reports [22–27]. The promising development in the search for antitumour organotin(IV) compounds has been achieved with some triphenyltin(IV) carboxylates such as 3,6-dioxaheptanoate and 3,6,9-trioxadecanoate [28], 4-carboxybenzo-15-crown-5 and 4-carboxybenzo-18-crown-6 [28,29], steroidcarboxylate [30] and terebate [2,31,32] when screened in vitro against human tumour cell lines as per NCI protocol.

In this paper, we report on the synthesis, spectroscopic and structural characterization of some new di-*n*-butyltin(IV) complexes involving 5-[(*E*)-2-(aryl)-1-diazenyl]quinolin-8-olate ligands (Fig. 1). The solid-state structures of the complexes $^nBu_2Sn(L^3)_2$ (**3**), $^nBu_2Sn(L^4)_2$ (**4**), $^nBu_2Sn(L^5)_2$ (**5**), and $^nBu_2Sn(L^7)_2$ (**7**) have been determined using single-crystal X-ray crystallography in order to confer deeper insight into their coordination geometry. The coordination geometry of the tin atom of these complexes in solution has been deduced from ^{119}Sn NMR data in non-coordinating solvent, while the cleavage of the most labile bond in each molecule has been studied using ESI mass spectrometry. The di-*n*-butyltin(IV) complexes of the type $^nBu_2Sn(L)_2$ and $^nBu_2SnCl(L)$ were tested across a panel of human cell lines *viz*., WIDR (colon cancer), M19 MEL (melanoma), A498 (renal cancer), IGROV (ovarian cancer) and H226 (non-small cell lung cancer), MCF7 (breast cancer), EVSA-T (breast cancer) to establish their activity.

2. Experimental

2.1. Materials

$^nBu_2SnCl_2$ (Merck), $^nBu_2SnO$ (Fluka), 8-hydroxyquinoline (Merck) and the substituted anilines (reagent grade) were used without further purification. The solvents used in the reactions were of AR grade and dried using standard procedures. Benzene was distilled from sodium benzophenone ketyl.

2.2. Physical measurements

Carbon, hydrogen and nitrogen analyses were performed with a Perkin–Elmer 2400 series II instrument. IR spectra in the range 4000–400 cm^{-1} were obtained on a BOMEM DA-8 FT-IR spectrophotometer with samples investigated as KBr discs. The ^{1}H-, ^{13}C - and ^{119}Sn NMR spectra were recorded on a Bruker AMX 400 spectrometer and measured at 400.13, 100.62 and 149.18 MHz, respectively. The ^{1}H, ^{13}C and ^{119}Sn chemical shifts were referred to Me_4Si set at 0.00 ppm, $CDCl_3$ set at 77.0 ppm and Me_4Sn set at 0.00 ppm, respectively. The splitting of proton resonances in the reported proton NMR spectra are defined as s = singlet, d = doublet, t = triplet, and m = multiplet. Positive-ion and negative-ion electrospray ionization (ESI) mass spectra were measured on an ion trap analyzer Esquire 3000 (Bruker Daltonics, Bremen, Germany) in the range *m*/*z* 50–1500. The samples were dissolved in 100% acetonitrile and analyzed by direct infusion at a flow rate of 5 μl/min. The selected precursor ions were further analyzed by MS/MS analyses under the following conditions: an isolation width of *m*/*z* = 8, a collision amplitude in the range 0.8–1.0 V depending on the precursor ion stability, an ion source temperature of 300° C, a tuning parameter for compound stability of 100%, while the flow rate and the pressure of nitrogen were 4 l/min and 10 psi, respectively [33,34]. The Mössbauer spectra of the complexes in the solid state were recorded using a Model MS-900 (Ranger Scientific Co., Burleson, TX) spectrometer in the acceleration mode with a moving source geometry. A 10 mCi $Ca^{119m}SnO_3$ source was used, and counts of 30,000 or more were accumulated for each spectrum. The spectra were measured at 80 K using a liquid-nitrogen cryostat (CRYO Industries of America, Inc., Salem, NH). The velocity was calibrated at ambient temperature using a composition of $BaSnO_3$ and tin foil (splitting 2.52 mm s^{-1}). The resultant spectra were analyzed using the Web Research software package (Web Research Co., Minneapolis, MN).

2.3. Synthesis of 5-[(E)-2-(aryl)-1-diazenyl)quinolin-8-ols

The 5-[(*E*)-2-(aryl)-1-diazenyl)quinolin-8-ols, L^1H–L^7H, used for synthesizing the di-*n*-butyltin(IV) complexes **1–7** were prepared by the method described earlier [12,13].

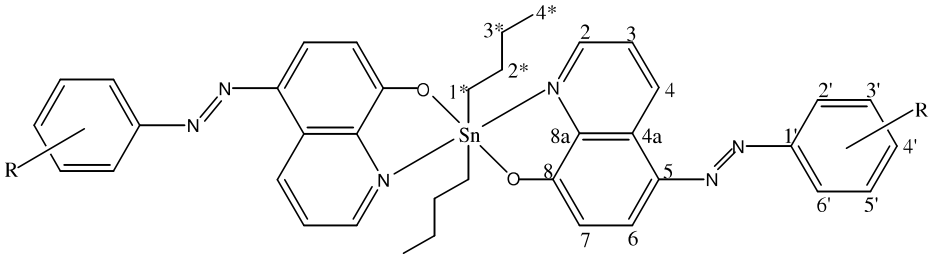

Fig. 1. Structure of the di-*n*-butyltin complexes (**1–7**) (Abbreviations: L^1: R = 2′-CH_3; L^2: R = 3′-CH_3; L^3: R = 4′-CH_3; L^4: R = 4′-OCH_3; L^5: R = 4′-OC_2H_5; L^6: R = 4′-Cl; L^7: R = 4′-Br).

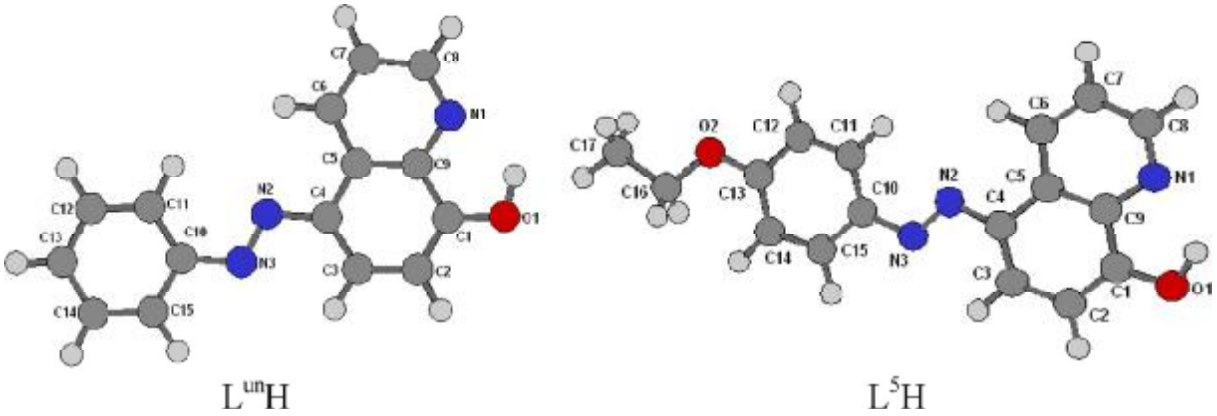

Fig. 2. The structures of the ligands $L^{un}H$ and L^5H obtained after full geometry optimization at DFT level (refer to the supplementary materials for the structures of other ligands L^3H, L^4H, L^6H, L^7H).

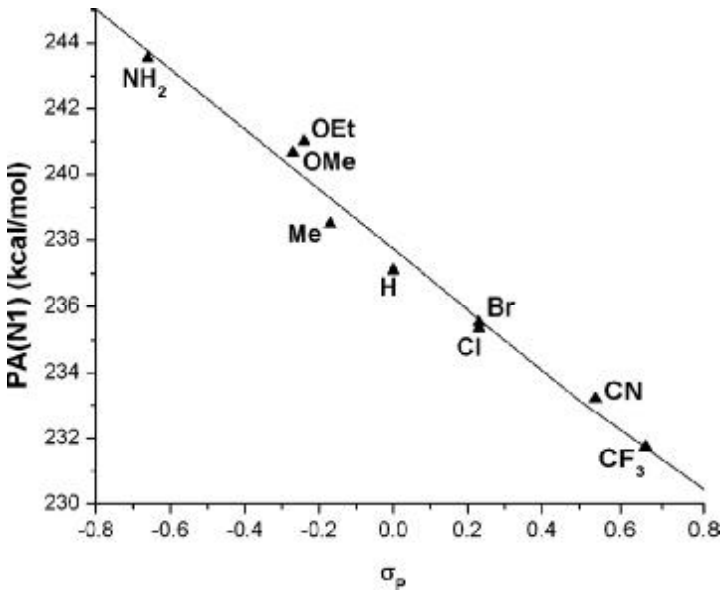

Fig. 3. A plot of proton affinity (PA) of the N(1) atom of the ligands (*para*-substituents) against Hammett's substituent constants (σ_P).

2.4. Synthesis of the di-n-butyltin(IV) complexes

2.4.1. Synthesis of $^nBu_2Sn(L^1)_2$ (**1**)

A methanolic solution of sodium methoxide (generated *in situ* from 0.045 g, 1.95 mmol of Na in anhydrous methanol) was added drop-wise into a stirred hot anhydrous benzene solution (45 ml) containing L^1H (0.5 g, 1.90 mmol). After the addition, a precipitate appears and the stirring was continued for an additional 15 min. To this reaction mixture, an anhydrous benzene solution (15 ml) of $^nBu_2SnCl_2$ (0.26 g, 0.85 mmol) was added drop-wise which resulted in the formation of NaCl. The reaction mixture was refluxed for 3 h and filtered to remove the NaCl. The filtrate was collected and the solvent was removed under reduced pressure. The resultant residue was extracted with hexane. The crude product was recrystallized from hexane, which upon cooling afforded a maroon coloured crystalline product. Yield: 0.35 g (53.8%), mp: 64–65 °C. Anal. found: C, 63.32; H, 5.78; N, 10.89%. Calc. for $C_{40}H_{42}N_6O_2Sn$: C, 63.42; H, 5.58; N, 11.09%. IR (cm^{-1}): 1248 ν(C(aryl)O. ^1H NMR ($CDCl_3$) δ_H: Ligand skeleton: 9.33 [dd, 1H, H4], 8.53 [dd, 1H, H2], 8.22 [d, 1H, H6], 7.68 [d, 1H, H6′], 7.35 [m, 4H, H3, H3′, H4′ and H5′], 7.26 [d, 1H, H7] and 2.75 [s, 3H, CH_3]; Sn–^{n}Bu skeleton: 1.45 [m, 4H, H1*], 1.25 [m, 8H, H2* and H3*], 0.78 [t, 6H, H4*] ppm. ^{13}C NMR ($CDCl_3$); δ_C: 162.2 [C8], 151.4 [C1′], 143.0 [C2], 137.3 [C5], 136.5 [C8a], 135.6 [C2′], 131.2 [C4], 129.8 [C3′], 128.7 [C4a], 126.3 [C4′], 122.3 [C5′], 118.9 [C3′], 115.5 [C6 and C6′], 114.1 [C7], 17.6 [CH_3]; Sn–^{n}Bu skeleton: 27.7 [C2*], 26.7 [C3*], 26.1 [C1*], 13.6 [C4*] ppm. ^{119}Sn NMR ($CDCl_3$) δ_{Sn}: −249.8 ppm. ^{119}Sn Mössbauer: $\delta = 1.00$, $\Delta = 2.33$, $\Gamma_1 = 1.84$, $\Gamma_2 = 1.98$ mm s^{-1}. MW = 758. Positive-ion ESI mass spectra: *m*/*z* 781 $[M + Na]^+$; *m*/*z* 496 $[M–L^1]^+$, 100%. MS/MS of 781: *m*/*z* 496 $[M–L^1]^+$; *m*/*z* 382 $[M–L^1–butene–butane]^+$. MS/MS of 496: *m*/*z* 438 $[M–L^1–butane]^+$; *m*/*z* 382 $[M–L^1–butene–butane]^+$. Negative-ion ESI mass spectra: *m*/*z* 262 $[L^1]^-$, 100%. MS/MS of 262: *m*/*z* 234 $[L^1–N_2]^-$; *m*/*z* 143 $[L^1–CH_3C_6H_4N_2]^-$.

The other di-*n*-butyltin complexes, **2–7**, were prepared by reacting the appropriate ligands, *viz*., L^2H–L^7H with $^nBu_2SnCl_2$ according to the procedure described above. The characterization and spectroscopic data of the complexes are presented below.

*2.4.2. $^{n}Bu_2Sn(L^2)_2$ (**2**)*

Maroon crystals of **2** were obtained from hexane. Yield: 0.33 g (50.7%), mp: 80–82 °C. Anal. found: C, 63.40; H, 5.53; N, 11.01%. Calc. for $C_{40}H_{42}N_6O_2Sn$: C, 63.42; H, 5.58; N, 11.09%. IR(cm^{-1}): 1253 ν(C(aryl)O). ^{1}H NMR ($CDCl_3$) δ_H: Ligand skeleton: 9.31 [dd, 1H, H4], 8.54 [dd, 1H, H2], 8.23 [d, 1H, H6], 7.72 [m, 2H, H2′ and H6′], 7.37 [m, 3H, H3, H4′ and H5′], 7.24 [d, 1H, H7] and 2.45 [s, 3H, CH_3]; Sn–^{n}Bu skeleton: 1.44 [m, 4H, H1*], 1.24 [m, 8H, H2* and H3*], 0.77 [t, 6H, H4*] ppm. ^{13}C NMR ($CDCl_3$); δ_C: 162.3 [C8], 153.5 [C1′], 143.1 [C2], 138.8 [C5], 136.1 [C3′], 135.7 [C8a], 135.5 [C4], 130.7 [C4′], 128.8 [C5′], 123.3 [C4a], 122.9 [C2′], 122.3 [C3], 119.8 [C6′], 118.7 [C6], 114.1 [C7], 21.4 [CH_3]; Sn–^{n}Bu skeleton: 27.7 [C2*], 26.7 [C3*], 26.1 [C1*], 13.6 [C4*] ppm. ^{119}Sn NMR ($CDCl_3$) δ_{Sn}: −249.6 ppm. ^{119}Sn Mössbauer: δ = 0.99, Δ = 2.43, Γ_1 = 2.00, Γ_2 = 2.00 mm s^{-1}. MW = 758. Positive-ion and negative-ion ESI mass spectra were identical as for **1**.

*2.4.3. $^{n}Bu_2Sn(L^3)_2$ (**3**)*

Red crystals of **3** were obtained from a mixture of benzene and hexane (v/v 1:1). Yield: 0.40 g (61.5%), mp: 171–172 °C. Anal. found: C, 63.40; H, 5.56; N, 11.05%. Calc. for $C_{40}H_{42}N_6O_2Sn$: C, 63.42; H, 5.58; N, 11.09%. IR (cm^{-1}): 1247 ν(C(aryl)O). ^{1}H NMR ($CDCl_3$) δ_H: Ligand skeleton: 9.28 [dd, 1H, H4], 8.54 [dd, 1H, H2], 8.21 [d, 1H, H6], 7.82 [d, 2H, H2′ and H6′], 7.33 [m, 4H, H3, H3′, H5′and H7], and 2.40 [s, 3H, CH_3]; Sn–^{n}Bu skeleton: 1.44 [m, 4H, H1*], 1.24 [m, 8H, H2* and H3*], 0.77 [t, 6H, H4*] ppm. ^{13}C NMR ($CDCl_3$); δ_C: 162.1 [C8], 151.5 [C1′], 143.0 [C2], 140.3 [C4′], 136.1 [C5], 135.7 [C8a], 135.5 [C4], 129.7 [C3′ and C5′] 128.6 [C4a], 122.4 [C2′ and C6′], 122.2 [C3], 118.4 [C6], 114.0 [C7], 21.4 [CH_3]; Sn-^{n}Bu skeleton: 27.7 [C2*], 26.8 [C3*], 26.1 [C1*], 13.6 [C4*] ppm. ^{119}Sn NMR ($CDCl_3$) δ_{Sn}: −249.8 ppm. ^{119}Sn Mössbauer: δ = 0.88, Δ = 2.04, Γ_1 = 1.79, Γ_2 = 2.00 mm s^{-1}. MW = 758. Positive-ion and negative-ion ESI mass spectra were identical as for **1**.

*2.4.4. $^{n}Bu_2Sn(L^4)_2$ (**4**)*

Orange crystals of **4** were obtained from a mixture of benzene and hexane (v/v 1:1). Yield: 0.47 g (69.6%), mp: 154–56° C. Anal. found: C, 60.83; H, 5.33; N, 10.62%. Calc. for $C_{40}H_{42}N_6O_4Sn$: C, 60.85; H, 5.36; N, 10.64%. IR (cm^{-1}): 1256 ν(C(aryl)O). ^{1}H NMR ($CDCl_3$) δ_H: Ligand skeleton: 9.26 [dd, 1H, H4], 8.53 [d, 1H, H2], 8.19 [d, 1H, H6], 7.92 [d, 2H, H6′ and H2′], 7.33 [m, 2H, H3 and H7], 7.03 [m, 2H, H3′ and H5′] and 3.88 [s, 3H, OCH_3]; Sn–^{n}Bu skeleton: 1.43 [m, 4H, H1*], 1.26 [m, 8H, H2* and H3*], 0.78 [t, 6H, H4*] ppm. ^{13}C NMR ($CDCl_3$); δ_C: 161.7 [C8], 161.3 [C1′], 147.8 [C4′], 142.9 [C2], 136.2 [C5], 135.5 [C8a], 135.5 [C4], 128.5 [C4a], 124.2 [C3′ and C5′], 122.1 [C3], 118.1 [C6], 114.2 [C2′ and C6′], 114.0 [C7], 55.5 [OCH_3]; Sn–^{n}Bu skeleton: 27.8 [C2*], 26.8 [C3*], 26.1 [C1*], 13.6 [C4*] ppm. ^{119}Sn NMR ($CDCl_3$) δ_{Sn}: −250.3 ppm. ^{119}Sn Mössbauer: δ = 0.93, Δ = 2.04, Γ_1 = 2.00, Γ_2 = 1.85 mm s^{-1}. MW = 790. Positive-ion ESI mass spectra: *m/z* 829 $[M+K]^+$; *m/z* 813 $[M+Na]^+$; *m/z* 512 $[M-L^4]^+$, 100%; *m/z* 398 $[M-L^4-butene-butane]^+$. MS/MS of 829: *m/z* 512 $[M-L^4]^+$; *m/z* 398 $[M-L^4$-butene-butane$]^+$. MS/MS of 813: *m/z* 512 $[M-L^4]^+$; *m/z* 398 $[M-L^4-butene-butane]^+$. MS/MS of 512: *m/z* 454 $[M-L^4-butane]^+$; *m/z* 398 $[M-L^4-butene-butane]^+$. Negative-ion ESI mass spectra: *m/z* 278 $[L^4]^-$; *m/z* 263 $[L^4-CH_3]^-$ 100%. MS/MS of 278: *m/z* 263 $[L^4-CH_3]^-$; *m/z* 235 $[L^4-CH_3-N_2]^-$; *m/z* 209. MS/MS of 263: *m/z* 235 $[L^4-CH_3-N_2]^-$.

*2.4.5. $^{n}Bu_2Sn(L^5)_2$ (**5**)*

Red crystals of **5** were obtained from a mixture of benzene and hexane (v/v 1:1). Yield: 0.57 g (82.7%), mp: 275–276° C. Anal. found: C, 61.66; H, 5.63; N, 10.26%. Calc. for $C_{42}H_{46}N_6O_4Sn$: C, 61.70; H, 5.67; N, 10.28%. IR (cm^{-1}): 1244 ν(C(aryl)O). ^{1}H NMR ($CDCl_3$) δ_H: Ligand skeleton: 9.25 [dd, 1H, H4], 8.52 [dd, 1H, H2], 8.17 [d, 1H, H6], 7.88 [m, 2H, H2′ and H6′], 7.32 [m, 2H, H3 and H7], 6.97 [m, 2H, H3′ and H5′], 4.09 [q, 2H, OCH_2CH_3] and 1.45 [t, 3H, OCH_2CH_3]; Sn–^{n}Bu skeleton: 1.45 [m, 4H, H1*], 1.24 [m, 8H, H2* and H3*], 0.76 [t, 6H, H4*]ppm. ^{13}C NMR ($CDCl_3$); δ_C: 161.6 [C8], 160.7 [C1′], 147.6 [C4′], 142.9 [C2], 136.1 [C5], 135.7 [C8a], 135.4 [C4], 128.5 [C4a], 124.1 [C3′ and C5′], 122.0 [C3], 118.0 [C6], 114.6 [C2′ and C6′], 113.9 [C7], 63.7 [OCH_2CH_3] and 14.7 [OCH_2CH_3]; Sn–^{n}Bu skeleton: 27.7 [C2*], 26.7 [C3*], 26.0 [C1*], 13.6 [C4*] ppm. ^{119}Sn NMR ($CDCl_3$) δ_{Sn}: −250.6 ppm. ^{119}Sn Mössbauer: δ = 0.95, Δ = 2.10, Γ_1 = 1.60, Γ_2 = 1.73 mm s^{-1}. MW = 818. Positive-ion ESI mass spectra: *m/z* 857 $[M+K]^+$; *m/z* 841 $[M+Na]^+$; *m/z* 526 $[M-L^5]^+$, 100%; *m/z* 412 $[M-L^5-butene-butane]^+$. MS/MS of 857: *m/z* 526 $[M-L^5]^+$; *m/z* 412 $[M-L^5-butene-butane]^+$. MS/MS of 841: *m/z* 526 $[M-L^5]^+$; *m/z* 412 $[M-L^5-butene-butane]^+$. MS/MS of 526: *m/z* 412 $[M-L^5-butene-butane]^+$. MS/MS of 412: *m/z* 354 $[M-L^5-butene-butane-ethane-N_2]^+$. Negative-ion ESI mass spectra: *m/z* 292 $[L^5]^-$; *m/z* 263 $[L^5-C_2H_5]^-$, 100%. MS/MS of 292: *m/z* 263 $[L^5-C_2H_5]^-$; *m/z* 235 $[L^5-C_2H_5-N_2]^-$; *m/z* 209. MS/MS of 263: *m/z* 235 $[L^5-C_2H_5-N_2]^-$.

*2.4.6. $^{n}Bu_2Sn(L^6)_2$ (**6**)*

Dark-red crystals of **6** were obtained from hexane. Yield: 0.59 g (85.3%), mp: 84–85° C. Anal. found: C, 57.13; H, 4.52; N, 10.45%. Calc. for $C_{38}H_{36}N_6O_2Cl_2Sn$: C, 57.16; H, 4.54; N, 10.52%. IR (cm^{-1}): 1257 ν(C(aryl)O). ^{1}H NMR ($CDCl_3$) δ_H: Ligand skeleton: 9.25 [dd, 1H, H4], 8.54 [dd, 1H, H2], 8.23 [d, 1H, H6], 7.82 [d, 2H, H2′ and H6′], 7.45 [d, 2H, H3′ and H5], 7.26 [m, 2H, H3 and H7]; Sn–^{n}Bu skeleton: 1.43 [m, 4H, H1*], 1.26 [m, 8H, H2* and H3*], 0.78 [t, 6H, H4*] ppm. ^{13}C NMR ($CDCl_3$); δ_C: 162.8 [C8], 151.8 [C1′], 143.1 [C2], 135.9 [C4′], 135.7 [C5], 135.6 [C8a], 135.5 [C4], 129.2 [C3′ and C5′], 128.8 [C4a], 123.6 [C2′ and C6′], 122.4 [C3], 119.0 [C6], 114.2 [C7], Sn–^{n}Bu skeleton: 27.7 [C2*], 26.7 [C3*], 26.2 [C1*], 13.5 [C4*] ppm. ^{119}Sn NMR ($CDCl_3$) δ_{Sn}: −248.5 ppm. ^{119}Sn Mössbauer: δ = 0.96, Δ = 2.21, Γ_1 = 1.88, Γ_2 = 2.00 mm s^{-1}. MW = 798. Positive-ion ESI mass spectra: *m/z* 837 $[M+K]^+$; *m/z* 821 $[M+Na]^+$; *m/z* 516 $[M-L^6]^+$, 100%; *m/z* 402 $[M-L^6-butene-butane]^+$. MS/MS of 821: *m/z* 516 $[M-L^6]^+$; *m/z* 404 $[M-L^6-2*butene]^+$. MS/MS of 516: *m/z* 458 $[M-L^6-butane]^+$; *m/z* 402 $[M-L^6-butene-butane]^+$. Negative-ion ESI mass spectra: *m/z* 282 $[L^6]^-$, 100%.

*2.4.7. $^{n}Bu_2Sn(L^7)_2.0.5C_6H_6$ (**7**)*

Red crystals of **7** were obtained from a mixture of benzene and hexane (v/v 2:1). Yield: 0.56 g (83.6%), mp: 154–56° C. Anal. found: C, 53.13; H, 4.20; N, 9.07%. Calc. for $C_{41}H_{39}Br_2N_6O_2Sn$: C, 53.16; H, 4.24; N, 9.07%. IR (cm^{-1}): 1247 ν(C(aryl)O). ^{1}H NMR ($CDCl_3$) δ_H: Ligand skeleton: 9.25 [dd, 1H, H4], 8.53 [dd, 1H, H2], 8.24 [d, 1H, H6], 7.77 [d, 2H, H2′ and H6′], 7.60 [m, 2H, H3′ and H5′], 7.35 [d, 2H, H3 and H7]; Sn–^{n}Bu skeleton: 1.43 [m, 4H, H1*], 1.26 [m, 8H, H2* and H3*], 0.75 [t, 6H, H4*] ppm. ^{13}C NMR ($CDCl_3$); δ_C: 162.8 [C8], 152.2 [C1′], 143.2 [C2], 135.9 to 135.5 [C4′, C5, C8a and C4], 132.2 [C3′ and C5′], 128.8 [C4a], 123.8 [C2′ and C6′], 122.4 [C3], 119.1 [C6], 114.2 [C7]; Sn–^{n}Bu skeleton: 27.7 [C2*], 26.7 [C3*], 26.2 [C1*], 13.5 [C4*] ppm. ^{119}Sn NMR ($CDCl_3$) δ_{Sn}: −248.2 ppm. ^{119}Sn Mössbauer: δ = 0.69, Δ = 2.07, Γ_1 = 2.00, Γ_2 = 2.00 mm s^{-1}. MW = 886. ESI mass spectrometric results are related to the unsolvated $^{n}Bu_2Sn(L^8)_2$ molecule. The presence of C_6H_6 is not observed in the mass spectra. Positive-ion ESI mass spectra: *m/z* 909 $[M+Na]^+$; *m/z* 560 $[M-L^7]^+$, 100%; *m/z* 446 $[M-L^7-butene-butane]^+$. MS/MS of 909: *m/z* 560 $[M-L^7]^+$; *m/z* 446 $[M-L^7-butene-butane]^+$. MS/MS of 560: *m/z* 504 $[M-L^7-butane]^+$; *m/z* 446 $[M-L^7-butene-butane]^+$. Negative-ion ESI mass spectra: *m/z* 326 $[L^7]^-$, 100%.

*2.4.8. $^{n}Bu_2SnCl(L^4)$ (**8**)*

The chloro di-*n*-butyltin(IV) complex was prepared by dropwise addition of sodium methoxide (generated *in situ* from 0.04 g, 1.75 mmol of Na in 15 ml anhydrous methanol) into a stir-

red hot anhydrous benzene solution (45 ml) of the ligand L^4H (0.5 g, 1.79 mmol). Immediate precipitation of the sodium salt occurred and then the reaction mixture was stirred vigorously for an additional 15 min. To this reaction mixture, an anhydrous benzene solution (15 ml) of $^nBu_2SnCl_2$ (0.52 g, 1.71 mmol) was added dropwise. The reaction mixture was refluxed for 3 h and filtered to remove the NaCl. The filtrate was collected and the solvent was removed under reduced pressure. The resultant mass was washed several times with ice cold hexane. The crude product was recrystallized from a mixture of benzene and hexane (v/v 1:2) which afforded orange crystals of **8**. Yield: 0.48 g (48.45%), mp: 72–74° C. Anal. found: C, 52.71; H, 5.45; N, 7.3%. Calc. for $C_{24}H_{30}N_3O_2ClSn$: C, 52.73; H, 5.53; N, 7.69%. IR (cm^{-1}): 1259 ν(C(aryl)O). ^1H NMR ($CDCl_3$) δ_H: Ligand skeleton: 9.65 [dd, 1H, H4], 8.20 [d, 1H, H2], 7.95 [d, 3H, H6′, H6 and H2′], 7.74 [m, 1H, H3], 7.25 [m, 1H, H7], 7.03 [m, 2H, H3′ and H5′] and 3.92 [s, 3H, OCH_3]; Sn–^{n}Bu skeleton: 1.72 [m, 4H, H1*], 1.35 [m, 8H, H2* and H3*], 0.85 [t, 6H, H4*] ppm. ^{13}C NMR ($CDCl_3$); δ_C: 161.7 [C8], 160.8 [C1′], 147.6 [C2], 145.9 [C4′], 138.1 [C4], 136.5 [C5], 136.3 [C8a], 128.4 [C4a], 124.4 [C3′ and C5′], 122.3 [C3], 118.4 [C6], 115.6 [C7], 114.3 [C2′ and C6′], 55.6 [OCH_3]; Sn–^{n}Bu skeleton: 28.2 [C2*], 26.9 [C3*], 26.3 [C1*], 13.4 [C4*] ppm. ^{119}Sn NMR ($CDCl_3$) δ_{Sn}: - 104.1 ppm. ^{119}Sn Mössbauer: δ = 1.15, Δ = 2.51, Γ_1 = 1.80, Γ_2 = 1.96 mm s^{-1}. MW = 547. Positive-ion ESI mass spectra: *m/z* 586 $[M+K]^+$; *m/z* 570 $[M+Na]^+$; *m/z* 548 $[M+H]^+$; *m/z* 512 $[M-Cl]^+$, 100%. MS/MS of 586: *m/z* 512 $[M-Cl]^+$; *m/z* 548 $[M+H]^+$. MS/MS of 570: *m/z* 512 $[M-Cl]^+$. MS/MS of 548: *m/z* 512 $[M-Cl]^+$; *m/z* 490 $[M+H-butane]^+$; *m/z* 434 $[M+H-butene-butane]^+$. MS/MS of 512: *m/z* 454 $[M-Cl-butane]^+$; *m/z* 398 $[M-Cl-butene-butane]^+$. Negative-ion ESI mass spectra: *m/z* 278 $[L^4]^-$; *m/z* 263 $[L^4-CH_3]^-$100%. MS/MS of 278: *m/z* 263 $[L^4-CH_3]^-$; *m/z* 235 $[L^4-CH_3-N_2]^-$; *m/z* 209. MS/MS of 263: *m/z* 235 $[L^4-CH_3-N_2]^-$.

Refer to Fig. 1 for the numbering scheme of the ligand and Sn–^{n}Bu skeletons for the assignment of ^1H and ^{13}C NMR signals.

2.5. X-ray crystallography

Crystals of compounds **3–5** and **7** suitable for an X-ray crystal-structure determination were obtained from slow evaporation of benzene/hexane (v/v 1:1) solutions of the respective compounds. All measurements were made at 160 K on a Nonius KappaCCD diffractometer [35] with graphite-monochromated Mo Kα radiation (λ = 0.71073 Å) and an Oxford Cryosystems Cryostream 700 cooler. Data reduction was performed with HKL Denzo and Scalepack [36]. The intensities were corrected for *Lorentz* and polarization effects, and empirical absorption corrections based on the multi-scan method [37] were applied. Equivalent reflections were merged. The data collection and refinement parameters are given in Table 1, and views of the molecules (**3–5** and **7**) are shown in Figs. 4–7. The structures were solved by direct-methods using SHELXS97 [38] for **3** and **4**, and SIR92 [39] for **5** and **7**.

The asymmetric unit in **3** and **4** contains one molecule in a general position, plus two half molecules, each of which sits across a C_2-axis. In **3** and **4**, the butyl groups in each of the C_2-symmetric molecules are disordered. Two sets of equally occupied positions were defined for the atoms of each disordered symmetry-independent butyl group. Similarity restraints were applied to the chemically equivalent bond lengths and angles involving all disordered C-atoms, while neighbouring atoms within and between each conformation of the disordered butyl groups were restrained to have similar atomic displacement parameters.

The 4′-ethoxyphenyl group of one quinolinolato ligand in **5** is disordered over two conformations. Two sets of overlapping positions were defined for the atoms of the ethoxyphenyl group and the site occupation factor of the major conformation refined to 0.541(4). Similarity restraints analogous to those described for **3** were employed during the refinement.

In **7**, the asymmetric unit contains one molecule of the Sn-complex, plus one half of a molecule of benzene, which sits across a centre of inversion. The benzene molecule is highly disordered within its cavity and a reasonable model could not be developed. Therefore, the contribution of the solvent molecules to the intensity data was removed by using the *SQUEEZE* [40] routine of the *PLATON* [41] program. Omission of the solvent molecule from the model leaves one cavity of 212 $Å^3$ per unit cell, located at a centre of inversion. The number of electrons contributing to each void in the structure was calculated by the *SQUEEZE* routine to be approximately 38 e. This corresponds well with the electron count for one

Table 1
Crystal data, data collection parameters and refinement results for di-*n*-butyltin(IV) complexes **3–5** and **7**

	3	**4**	**5**	**7**
Empirical formula	$C_{40}H_{42}N_6O_2Sn$	$C_{40}H_{42}N_6O_4Sn$	$C_{42}H_{46}N_6O_4Sn$	$C_{38}H_{36}Br_2N_6O_2Sn \cdot 0.5(C_6H_6)$
Formula weight	757.41	789.41	817.46	926.21
Crystal size (mm)	0.17 × 0.20 × 0.25	0.10 × 0.25 × 0.30	0.17 × 0.20 × 0.35	0.10 × 0.25 × 0.30
Crystal color, shape	Red, prism	Orange, tablet	Red, prism	Red, tablet
Crystal system	Monoclinic	Monoclinic	Triclinic	Triclinic
Space group	*C*2/*c*	*C*2/*c*	$P\bar{1}$	$P\bar{1}$
a (Å)	35.8749(4)	37.6805(5)	9.4380(2)	11.3778(2)
b (Å)	21.8444(3)	20.7797(3)	13.8486(3)	11.7967(2)
c (Å)	23.1536(3)	19.4559(3)	15.5419(2)	16.0362(2)
α	90	90	99.069(1)	87.3218(8)
β (°)	126.1936(6)	106.7291(8)	97.614(1)	76.9184(8)
γ	90	90	92.793(1)	70.5888(7)
V ($Å^3$)	14643.2(3)	14589.0(4)	1983.26(7)	1976.41(6)
Z	16	16	2	2
D_x (g cm^{-3})	1.374	1.438	1.369	1.556
μ (mm^{-1})	0.740	0.750	0.692	2.716
Transmission factors (min, max)	0.719, 0.823	0.789, 0.930	0.748, 0.894	0.602, 0.771
$2\theta_{max}$ (°)	60	55	60	55
Reflections measured	184867	169908	60733	46102
Independent reflections (R_{int})	21411 (0.079)	16708 (0.092)	11577 (0.041)	9054 (0.058)
Reflections with $I > 2\sigma(I)$	11070	8881	10128	7060
Number of parameters	968	993	565	462
Number of restraints	78	52	254	51
$R(F)$ ($I > 2\sigma(I)$ reflns)	0.053	0.045	0.033	0.042
$wR(F^2)$ (all data)	0.177	0.145	0.076	0.115
$GOF(F^2)$	1.05	1.04	1.03	1.06
max, min $\Delta\rho$ (e/$Å^3$)	1.29, −2.94	1.70, −1.96	1.04, −0.90	1.23, −1.52

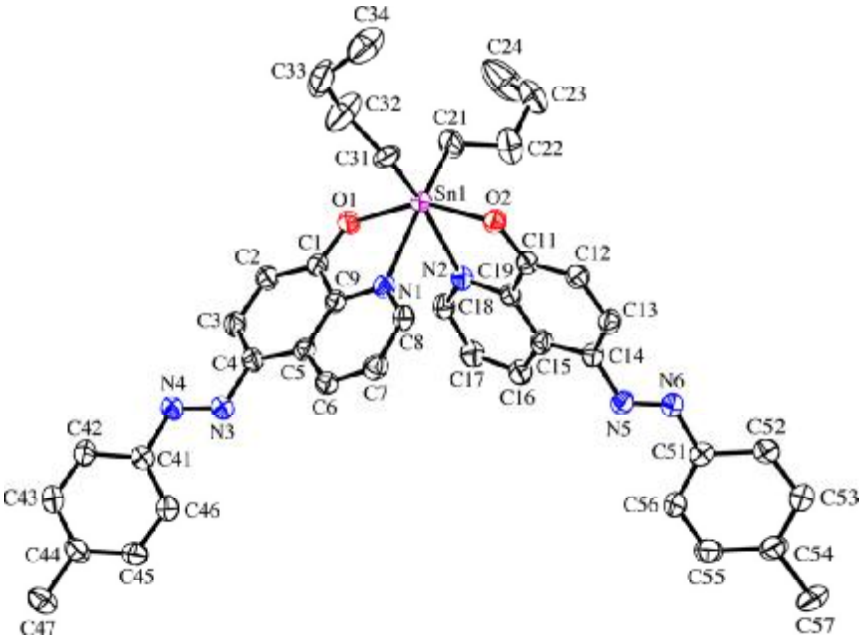

Fig. 4. The molecular structure of $^{n}Bu_2Sn(L^3)_2$ (**3**). Displacement ellipsoids are shown at the 50% probability level. Only one orientation of the disordered *n*-butyl group is shown.

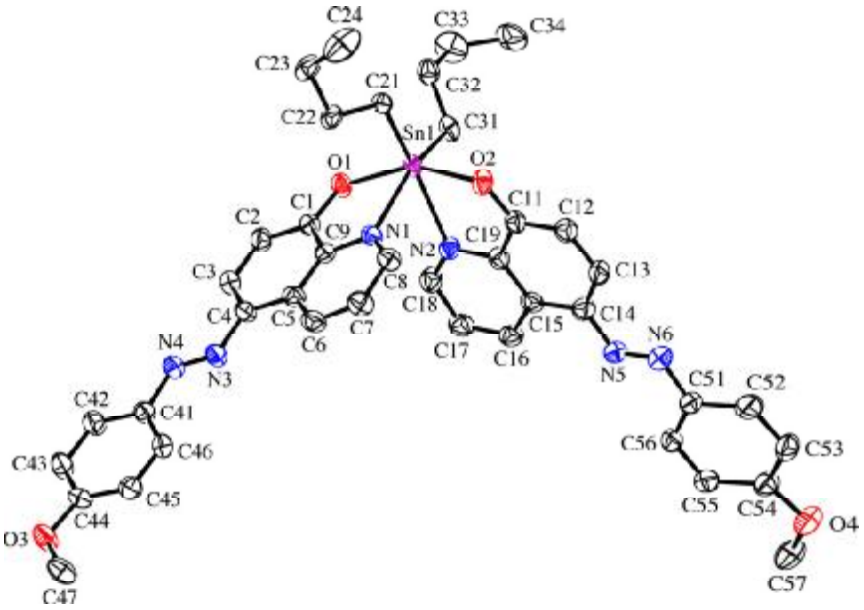

Fig. 5. The molecular structure of $^{n}Bu_2Sn(L^4)_2$ (**4**). Displacement ellipsoids are shown at the 50% probability level. Only one orientation of the disordered *n*-butyl group is shown.

molecule of benzene per cavity (42 e), which is consistent with the crystallization solvent (benzene/hexane) and the residual electron density peaks initially observed for this region of the structure. The assumed solvent composition was used in the subsequent calculation of the empirical formula, formula weight, density, linear absorption coefficient and $F(000)$. One of the butyl groups in **7** is disordered over two conformations. Two sets of overlapping positions were defined for central two methylene groups of the disordered butyl group and the site occupation factor of the major conformation refined to 0.776(7). Similarity restraints analogous to those described for **3** were employed during the refinement.

For each structure, the non-hydrogen atoms were refined anisotropically. All of the H-atoms were placed in geometrically calculated positions and refined by using a riding model where each H-atom was assigned a fixed isotropic displacement parameter with a value equal to $1.2U_{eq}$ of its parent C atom ($1.5U_{eq}$ for the methyl groups). The refinement of each structure was carried out on F^2 using full-matrix least-squares procedures, which min-

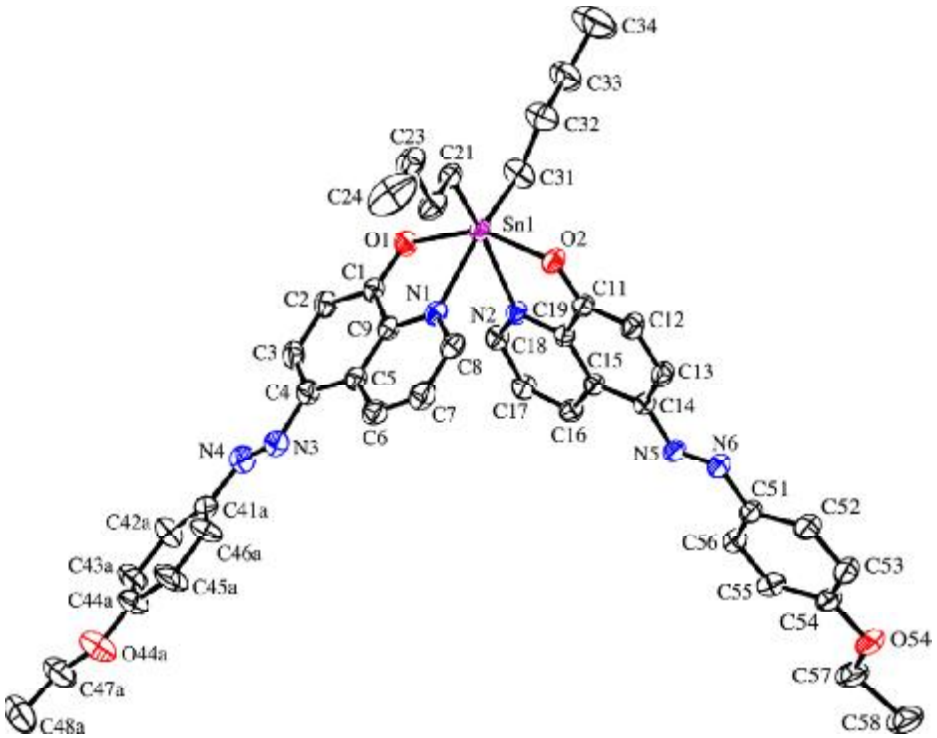

Fig. 6. The molecular structure of $^{n}Bu_2Sn(L^5)_2$ (**5**). Displacement ellipsoids are shown at the 50% probability level. Only one orientation of the disordered 4′-ethoxyphenyl group is shown.

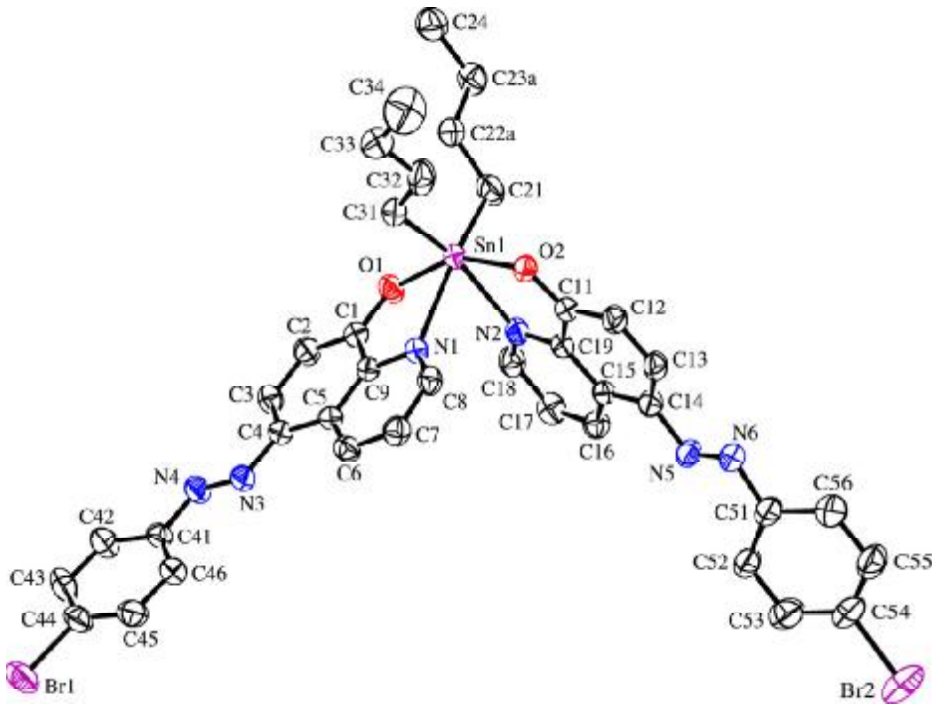

Fig. 7. The molecular structure of $^{n}Bu_2Sn(L^7)_2$ (**7**). Displacement ellipsoids are shown at the 50% probability level. Only one orientation of the disordered *n*-butyl group is shown.

imized the function $\Sigma w(F_o^2 - F_c^2)^2$. Corrections for secondary extinction were applied for **3** and **4**. Four reflections in **3**, six reflections in **4** and one reflection in **7**, whose intensities were considered to be extreme outliers, were omitted from the final refinement. All calculations were performed using the SHELXL97 program [42].

2.6. Biological tests

The *in vitro* cytotoxicity test of di-*n*-butyltin(IV) compounds **3–8** were performed using the SRB test for the estimation of cell viability. The cell lines WIDR (colon cancer), M19 MEL (melanoma), A498 (renal cancer), IGROV (ovarian cancer) and H226 (non-small cell lung cancer) are currently used in the anticancer screening panel at the National Cancer Institute of the National Institutes of Health, USA [43]. The MCF7 (breast cancer) cell line is estrogen receptor (ER)+/progesterone receptor (PgR)+ and the cell line EVSA-T (breast cancer) is (ER)−/(Pgr)−. Prior to the experiments, a mycoplasma test was carried out on all cell lines and found to be negative. All cell lines were maintained in a continuous logarithmic culture in RPMI 1640 medium with Hepes and phenol red. The medium was supplemented with 10% FCS, penicillin 100 μg/ml and streptomycin 100 μg/ml. The cells were mildly trypsinized for passage and for use in the experiments. RPMI and FCS were obtained from Life technologies (Paisley, Scotland). SRB, DMSO, Penicillin and streptomycin were obtained from Sigma (St. Louis MO, USA), TCA and acetic acid from Baker BV (Deventer, NL) and PBS from NPBI BV (Emmer-Compascuum, NL).

The test compounds **3–8** and reference compounds were dissolved to a concentration of 250,000 ng/ml in full medium, by 20-fold dilution of a stock solution which contained 1 mg of compounds/200 μl. Compounds **3**, **4** and **6** were dissolved in DMSO (dimethylsulfoxide) while compounds **5**, **7** and **8** did not dissolve completely in DMSO, and the suspension of the test compound in DMSO was used to make the appropriate dilutions in medium. Cytotoxicity was estimated by the microculture sulforhodamine B (SRB) test [44].

2.6.1. Experimental protocol and cytotoxicity tests

The experiment was started on day 0. On day 0, 10,000 cells per well were seeded into 96-wells flatbottom microtiter plates (falcon 3072, DB). The plates were incubated overnight at 37° C, 5% CO_2 to allow the cells to adhere to the bottom. On day 1, a three-fold dilution sequence of ten steps was made in full medium, starting with the 250,000 ng/ml stock solution. Every dilution was used in quadruplicate by adding 200 μl to a column of four wells. This procedure results in the highest concentration of 625,000 ng/ml being present in column 12. Column 2 was used for the blank. After incubation for 3 days, the plates were washed with PBS twice. Fluorescein diacetate (FDA) stock solution was diluted to 2 μg/ml with PBS and 200 μl of this solution was added to each of the control, experimental and blank wells. The plates were incubated for 30 min at 37° C and the fluorescence generated from each well was measured at an excitation wavelength of 485 nm and an emission wavelength of 535 nm using an automated microplate reader (Labsystems Multiskan MS). The data were used for the construction of concentration–response curves and the determination of the ID_{50} value by use of the Deltasoft 3 software. ID_{50} value represents the inhibitory dose in ng/ml measured from the fluorescence indicating a cell kill of 50%.

The variability of the *in vitro* cytotoxicity test depends on the cell lines used and the serum applied. With the same batch of cell lines and the same batch of serum the interexperimental CV (coefficient of variation) is 1–11% depending on the cell line and the intraexperimental CV is 2–4%. These values may be higher with other batches of cell lines and/or serum.

2.7. Quantum chemical calculations

The geometries of the unsubstituted ligand ($L^{un}H$) and *para*-substituted ligands, viz., L^3H–L^7H were optimized using the B3LYP [45] density functional theory (DFT) method with the 6-31G(d) basis set. Harmonic frequency calculations were performed at all the stationary points to characterize its nature and to ensure that the optimized structure corresponds to a global minimum. The optimized structures of an unsubstituted ligand ($L^{un}H$) and a representative *para*-substituted ligand (L^5H) are shown in Fig. 2 while the geometric parameters for $L^{un}H$, L^3H–L^7H are listed in Table 2. The basicity of the N(1) atom of the ligand and the O(1) atom of the corresponding anion generated after removal of the H-atom of the O(1)H group is estimated from the proton affinity of the N(1) atom [PA (N(1))] and the O(1) atom [PA (O(1))]. The PA for a base (B) is defined as the negative of the enthalpy (H) change for the reaction:

$$B + H^+ \rightarrow BH^+$$

Therefore, at any finite temperature (T) the PA can be estimated from the expression:

$$PA = H(B) + H(H^+) - H(BH^+)$$

At 0 K, $H(H^+)$ can be taken as zero and H(B) = E(B), where E(B) is the energy of base B at 0 K. In the present calculations, the PA values at 0 K were estimated simply from the total energies calculated

Table 2
Selected bond lengths (Å), angles (°), and torsion angles (°) for optimized structures (B3LYP/6-31G(d)) of ligands ($L^{un}H$, L^3H–L^7H)[a] and the proton affinity (PA in kcal/mol) values for the N(1) atom of L–H and $O(1)^-$ atom of LO^- anion

Bond lengths (Å)/angles (°)	$L^{un}H$	L^3H	L^4H	L^5H		L^6H	L^7H
				(Calc.)	(Expt.)[b]		
O(1)–C(1)	1.344	1.344	1.345	1.345	1.352(2)	1.343	1.343
O(2)–C(13)	–	1.509[c]	1.361	1.359	1.362(3)	–	–
O(2)–C(16)	–	–	1.420	1.429	1.429(2)	–	–
N(1)–C(8)	1.319	1.319	1.319	1.319	1.312(3)	1.319	1.319
N(1)–C(9)	1.360	1.360	1.360	1.361	1.366(2)	1.360	1.360
N(2)–N(3)	1.265	1.265	1.266	1.266	1.262(2)	1.266	1.266
N(2)–C(4)	1.405	1.406	1.406	1.406	1.422(3)	1.403	1.403
N(3)–C(10)	1.415	1.413	1.408	1.408	1.418(3)	1.413	1.413
C(1)–C(2)	1.387	1.387	1.386	1.386	1.367(3)	1.387	1.387
C(1)–C(9)	1.431	1.430	1.430	1.429	1.419(3)	1.431	1.431
O(1)–H	0.984	0.984	0.984	0.984	–	0.984	0.984
C(9)–N(1)–C(8)	117.8	118.0	117.8	117.8	116.97(19)	117.8	117.8
O(1)–C(1)–C(9)	118.4	118.4	118.4	121.8	120.86(19)	118.4	118.4
C(4)–N(2)–N(3)–C(10)	−179.8	−179.9	180.0	−179.9	−179.24(18)	179.9	180.0
PA (N(1))	237.1	238.5	240.6	241.0	–	235.4	235.5
PA ($O(1)^-$)	342.2	343.3	344.9	345.0	–	338.6	338.5

[a] Refer to Fig. 2 for numbering scheme.
[b] Data taken from Ref. [13].
[c] C(13)–C(16) distance.

at the B3LYP/6-311G(d,p)//6-31G(d) level: PA(N(1)) = E(L–H) – E(L–H–NH$^+$) and PA(O(1)) = E(L–O$^-$) – E(L–H). In the present study, the main aim is to calculate relative PA values for the ligands and for this purpose, the B3LYP method [46,47] was used which is known to produce reliable PA values. Gaussian-03 program was used for all the electronic structure calculations [48].

3. Results and discussion

3.1. Optimized structures of ligands ($L^{un}H$, L^3H–L^7H) and the proton affinity for the N(1) atom of L–H and the O(1)$^-$ atom of LO$^-$ anion

The optimized structures for the ligands ($L^{un}H$ and L^5H) are shown in Fig. 2 while the geometrical parameters for $L^{un}H$, L^3H–L^7H along with the proton affinity for the N(1) atom of L–H and the O(1)$^-$ atom of the LO$^-$ anion are listed in Table 2. The X-ray experimental geometric parameters for L^5H are also included in Table 2 along with calculated values for comparison. The calculated values agree well with the experimental data. Most of the geometric parameters are found to be insensitive to the nature of the substituents. However, the substituents can have a strong effect on the basicity of donor atoms, as discussed later. Since the basic structures of the di-*n*-butyltin(IV) complexes (**1–7**) are similar for the differently substituted ligands, it can be expected that the ligand properties will have direct influences on the stability of the corresponding di-*n*-butyltin(IV) complexes, as well as on their cytotoxic activity (see Section 3.5). As the O(1) and N(1) atoms of the ligands act as donor atoms to bind with the Sn-atom, we further investigated how the basicity of these two atoms changes with the change in substituents. The proton affinity values (Table 2) for both the N(1) and O(1) atoms increase for the electron donor substituents (such as Me (in L^3H), OMe (in L^4H), and OEt (in L^5H)), while it decreases for the electron withdrawing substituents when compared with the unsubstituted ligand ($L^{un}H$). A good correlation is observed between the proton affinities for the N(1) atom of the ligands and the O(1) atom of the corresponding anions and Hammett's parameters (σ_P) [49] for different remote substituents. A correlation between PA(N(1)) and σ_P are shown in Fig. 3. Ligands with the –NH_2, –CN and –CF_3 substituents are also included in the correlation to increase the breadth of this comparison.

3.2. Syntheses

The di-*n*-butyltin(IV) complexes of 5-[(*E*)-2-(aryl)-1-diazenyl]quinolin-8-ol were prepared by reacting stoichiometric amounts of $^nBu_2SnCl_2$ and LNa (generated *in situ* from Na and anhydrous methanol) in anhydrous benzene (Eq. (1)) using the procedure described for the dibenzyltin(IV) analogues [12]. The di-*n*-butyltin(IV) complexes (**1–7**) could also be prepared by reacting $^nBu_2SnO$ with LH in 1:2 molar ratios using a Dean–Stark apparatus in toluene (Eq. (2)) and in some cases, the yields were better. The work-up convenience and purity considerations led to the choice of Eq. (1). On the other hand, $^nBu_2SnCl(L^4)$ (**8**) was obtained by the reaction of $^nBu_2SnCl_2$ and L^4Na in an equimolar ratio in anhydrous benzene (Eq. (3)). The work-up details and characterization data for the complexes are described in Section 2.4.

$$2L^{1-7}H + 2NaOMe + {}^nBu_2SnCl_2 \xrightarrow[\text{Reflux,3 h}]{\text{Benzene}} {}^nBu_2Sn(L^{1-7})_2 + 2MeOH + 2NaCl \quad (1)$$

$$2L^{1-7}H + {}^nBu_2SnO \xrightarrow[\text{Reflux,3 h}]{\text{Toluene}} {}^nBu_2Sn(L^{1-7})_2 + H_2O \quad (2)$$

$$L^4H + NaOMe + {}^nBu_2SnCl_2 \xrightarrow[\text{Reflux,3 h}]{\text{Benzene}} {}^nBu_2SnCl(L^4)_2 + MeOH + NaCl \quad (3)$$

The di-*n*-butyltin(IV) complexes could be isolated by fractional crystallization with high purity in moderate to good yield (51–85%). The complexes are crystalline in nature, stable in air and are soluble in all common organic solvents.

3.3. Structural results from single crystal X-ray diffraction

The results of the X-ray crystallographic study on complexes **3–5** and **7** (Figs. 4–7) are fully consistent with the other spectroscopic evidence described in Section 3.4. As a representative example, the selected geometric parameters of **5** are given in Table 3. The corresponding geometric parameters for the other complexes (**3**, **4** and **7**) have very similar values. The asymmetric unit of **3** and **4** contains one molecule in a general position, plus two half molecules, each of which sits across a C_2-axis. The butyl groups in the C_2-symmetric molecules are disordered. These two complexes crystallize in the same space group, have quite similar unit cell dimensions, and are close to isostructural. The ethoxyphenyl group of one bidentate ligand in **5** is disordered over two positions, which result primarily from a reversal of the direction of the zig-zag conformation of the ethoxy group. In **7**, the asymmetric unit contains one molecule of the Sn-complex, plus one half of a molecule of benzene, which sits across a centre of inversion. One of the butyl groups in this complex is disordered over two conformations.

The Sn-atom in all four complexes (**3–5** and **7**) has a distorted octahedral coordination geometry in which the O-atoms from the two bidentate ligands are approximately *trans* to one another, but *cis* to the two *n*-butyl ligands, while the quinolin-8-olate N-atoms are *trans* to the butyl groups. The small bite angle subtended by the donor atoms of the quinolin-8-olate moiety is the main reason for the distortion from a regular octahedral geometry. The metric parameters of these di-*n*-butyltin(IV) complex molecules closely match those of their diphenyltin(IV) and dibenzyltin(IV) analogues [12,13]. The Sn-coordination geometry is also very similar to that found in $^nBu_2Sn$(quinolin-8-olate)$_2$ and $^tBu_2Sn$(quinolin-8-olate)$_2$, which have more compact ligands [8]. Some variations are observed in the dihedral angle between the planes of the substituted phenyl ring and the quinolin-8-olate ring in each of the L ligands of **3–5** and **7**. Whereas these dihedral angles range from 37.0(2)° to 40.0(2)° among the four symmetry-independent L^3 ligands in **3**, the range across the four symmetry-independent L^4 ligands in **4** is only 6.0(2)° to 9.1(2)°, which indicates a much higher degree of coplanarity of these rings in **4**. In **5** and **7**, one L ligand is more twisted than the other, with the two dihedral angles being 11.2(1)° and 30.4(2)° for **5**, and 6.12(7)° and 21.9(2)° for **7**. In the related diphenyltin(IV) and dibenzyltin(IV) analogues [12,13], both nearly planar and slightly twisted arrangements of the L ligands were observed, with the dihedral angle between the planes of the substituted phenyl ring and the quinolin-8-olate ring varying from 5° to 20°.

Table 3
Selected bond lengths (Å) and angles (°) for $^nBu_2Sn(L^5)_2$ (**5**)

Sn(1)–C(21)	2.158(2)	O(2)–Sn(1)–N(1)	84.51(5)
Sn(1)–C(31)	2.150(2)	O(2)–Sn(1)–N(2)	72.94(5)
Sn(1)–O(1)	2.111(1)	O(1)–Sn(1)–O(2)	152.19(5)
Sn(1)–O(2)	2.103(1)	C(21)–Sn(1)–N(1)	92.05(7)
Sn(1)–N(1)	2.332(2)	C(21)–Sn(1)–N(2)	161.32(6)
Sn(1)–N(2)	2.396(1)	C(31)–Sn(1)–N(1)	158.10(7)
N(1)–C(9)	1.357(2)	C(31)–Sn(1)–N(2)	88.33(7)
N(2)–C(19)	1.365(2)	C(21)–Sn(1)–C(31)	108.28(8)
N(3)–N(4)	1.251(3)	O(1)–Sn(1)–C(21)	102.84(6)
N(5)–N(6)	1.264(2)	O(1)–Sn(1)–C(31)	93.34(7)
		O(2)–Sn(1)–C(21)	94.91(6)
O(1)–Sn(1)–N(1)	73.74(5)	O(2)–Sn(1)–C(31)	101.28(8)
O(1)–Sn(1)–N(2)	84.10(5)	N(1)–Sn(1)–N(2)	73.05(5)

3.4. Spectroscopy

The IR spectra of the ligands (L^1H–L^7H), and their diphenyltin(IV) and dibenzyltin(IV) complexes were described in our earlier communications [12,13]. The ν(OH) band is found to be absent in the IR spectra of di-*n*-butyltin(IV) complexes, **1–8**, confirming bonding through the O-atom of the ligand. A strong band at around 1250 cm^{-1}, is assigned to the ν(C(aryl)-O), i.e. C_8–O–Sn linkage in the complexes [12,13,50].

The ^1H and ^{13}C NMR data of L^1H–L^7H were also described earlier [12,13]. The conclusions drawn from the ligand assignments were then subsequently extrapolated to their complexes owing to their data similarity and it was possible to detect all proton and carbon signals for di-*n*-butyltin(IV) complexes **1–8** (see Section 2.4). The ^1H NMR integration values and the number of ^{13}C signals correspond with the proposed formulations of the products. The ^1H and ^{13}C chemical shift assignment of the di-*n*-butyltin(IV) moiety is straightforward from the multiplicity patterns and resonance intensities. The coordination number in solution was determined from the ^{119}Sn chemical shift and the $^1J(^{119}Sn–^{13}C)$ coupling constants of the *n*-butyl ligands, since tin shielding and the coupling constant both increase with coordination number. The ^{119}Sn NMR spectrum of each of the di-*n*-butyltin(IV) complexes studied displayed only one resonance signal for $^nBu_2Sn(L^{1–7})_2$ (**1–7**) at around −250 ppm and for $^nBu_2SnCl(L^4)$ (**8**) −104 ppm, in deuterochloroform solutions. The observed $\delta(^{119}Sn)$ chemical shifts for the chelated complexes (**1–8**) fall within the typical ranges for five (ca. −90 to −330 ppm) and six (ca. −125 to −515 ppm) coordinate derivatives [51]. The $\delta(^{119}Sn)$ values of complexes (**1–7**) are comparable with the shift observed for $^nBu_2Sn(quinolin\text{-}8\text{-}olate)_2$ (−262 ppm in $CHCl_3$ solution [51,52] and −260 in $CDCl_3$ [53]). The solution ^{119}Sn NMR shift of $^nBu_2Sn(quinolin\text{-}8\text{-}olate)_2$ was found to be comparable with that obtained from the solid state ^{119}Sn CP MAS NMR (−277 ppm), indicating that $^nBu_2Sn(quinolin\text{-}8\text{-}olate)_2$ possesses the same structure in solution and in the solid state [3]. This conclusion was subsequently confirmed for $^nBu_2Sn(quinolin\text{-}8\text{-}olate)_2$ by crystallography [8,54]. On the other hand, the $\delta(^{119}Sn)$ value for the chloro di-*n*-butyltin(IV) complex (**8**) corresponds well with that of $^nBu_2SnCl(quinolin\text{-}8\text{-}olate)$ (−112 ppm in $CHCl_3$ solution [51,55]). Furthermore, the $^1J(^{119}Sn–^{13}C)$ coupling constant values are around 625 Hz (**1–7**) and 590 Hz (**8**), which correspond well with the reported values [56,57]. On this basis, it is concluded that the $^nBu_2Sn(L^{1–7})_2$ complexes (**1–7**) are six-coordinate in solution, while $^nBu_2SnCl(L^4)$ (**8**) is a five coordinate species. Thus, the ^{119}Sn NMR data indicate that the complexes retain their solid-state structures in solution (see Mössbauer and crystal structure discussion).

The ^{119}Sn Mössbauer data i.e. isomer shift (δ), quadrupole splittings (Δ) and the line widths at half-peak height (Γ) for the di-*n*-butyltin(IV) complexes (**1–8**) are given in Section 2.4. In general, the complexes displayed a doublet with δ and Δ values in the range 0.69–1.15 and 2.04–2.51 mm s^{-1}, respectively. The observed Δ values for the $^nBu_2Sn(L^{1–7})_2$ complexes (**1–7**) lie within the range delimited for those diorganotin complexes which have a *cis*-R_2Sn octahedral geometry [58,59]. The values are in agreement with the data observed for the *cis*-octahedral $^nBu_2Sn(quinolin\text{-}8\text{-}olate)_2$ complex (Δ = 2.04 [60]) [8]. The magnitudes of the δ and Δ values in the complexes **1–7** are similar to each other, which would indicate that they are isostructural. Thus, the Mössbauer spectroscopic data suggest a *cis*-R_2Sn octahedral geometry for complexes **1–7**. On the other hand, the observed Δ value for $^nBu_2SnCl(L^4)$ (**8**) is 2.51 mm s^{-1}, which falls within the range observed for $R_2SnCl(quinolin\text{-}8\text{-}olate)$ complexes (R = alkyl or aryl, Δ range = 2.40–3.36 mm s^{-1}) [60] that have a trigonal bipyramidal geometry where the Cl and N atoms occupy the axial positions.

In the mass spectrometer, the main mechanism of ion formation is the cleavage of the most labile bond between tin and chloride or an organic ligand yielding two complementary ions, where the cationic part of the molecule is observed in the positive-ion mass spectra, i.e. $[M–L]^+$ or $[M–Cl]^+$, and the anionic part in the negative-ion mass spectra, i.e. $[L]^-$ [17,18,61]. The ion $[Cl]^-$ cannot be observed in the spectra because the *m*/*z* value of 35 is outside the instrument scan range. When both chlorides and an organic ligand are coordinated to the tin atom, the loss of chlorine is preferred. Other ions observed in the first-order positive-ion mass spectra are sodium and potassium ion adducts and in some cases protonated molecules. It is also noteworthy that the position of the methyl group on the ligand in $^nBu_2Sn(L^{1–3})_2$ complexes (**1–3**) has no influence on the ion formation and the same mass spectra were obtained for these three complexes. The tandem mass spectra of some important ions were recorded in order to obtain more structural information. The neutral losses of butane or butene confirm the presence of a butyl substituent on the tin atom and the loss of 28 (N_2) confirms the presence of an azo group in the molecule. Moreover, the loss of alkyl is observed in the spectra of complexes (**4**, **5** and **8**), which contain an alkoxy group. The molecular weight of all studied complexes can be confirmed from the information obtained from both positive-ion and negative-ion first-order spectra.

3.5. In vitro cytotoxicity

The results of the *in vitro* cytotoxicity test in human tumour cell lines on $^nBu_2Sn(L^{3–7})_2$ (**3–7**), $^nBu_2SnCl(L^4)$ (**8**) along with a diphenyltin(IV) complex $Ph_2Sn(L)_2$ (where L = 5-[(*E*)-2-(aryl)-1-diazenyl]quinolin-8-olate) are given as ID_{50} values in Table 4, and compared with the data for some compounds that are in current clinical use as antitumour agents. The table clearly shows that di-*n*-butyltin(IV) complexes (**3–7**) are overall, but not for every cell line, more active than cisplatin. The compounds **3**, **4** and **6** display the highest activity, even higher than several of the standard cytotoxic agents. All di-*n*-butyltin(IV) compounds show a dramatic increase in *in vitro* cytotoxicity compared with the related diphenyltin(IV) compound, $Ph_2Sn(L)_2$. However, the exact reasons for increased activity could not be inferred from the present data. A reverse trend i.e. an increase in activity from *n*-butyl to phenyl substituents has also been found (see Ref. [2], also for more information on structure–activity relationship).

Further, di-*n*-butyltin(IV) compounds (**3–7**) allow calculations on the structure activity relationship with respect to the substituents at the *para*-position of the diazo forming moiety of the ligand

Table 4
The ID_{50} values (ng/ml) of test compounds (**3–8**) *in vitro* (using as cell viability test) in seven human tumour cell lines

Test compound[a]	Cell lines						
	A498	EVSA-T	H226	IGROV	M19	MCF-7	WIDR
3	90	38	113	65	59	48	233
4	136	46	224	111	65	95	451
5	589	167	864	351	268	374	2064
6	248	85	407	395	72	143	1190
7	112	32	147	44	64	51	330
8	1605	527	1721	440	374	968	3680
$Ph_2Sn(L)_2$[b]	16902	8677	8950	4774	10104	7332	8441
DOX	90	8	199	60	16	10	11
CPT	2253	422	3269	169	558	699	967
5-FU	143	475	340	297	442	750	225
MTX	37	5	2287	7	23	18	<3.2
ETO	1314	317	3934	580	505	2594	150
TAX	<3.2	<3.2	<3.2	<3.2	<3.2	<3.2	<3.2

[a] Abbreviations: **3** = $^nBu_2Sn(L^3)_2$, **4** = $^nBu_2Sn(L^4)_2$, **5** = $^nBu_2Sn(L^5)_2$, **6** = $^nBu_2Sn(L^6)_2$, **7** = $^nBu_2Sn(L^7)_2$, **8** = $^nBu_2SnCl(L^4)$, DOX = doxorubicin, CPT = cisplatin, 5-FU = 5-fluorouracil, MTX = methotrexate, ETO = etoposide and TAX = paclitaxel.

[b] L = 5-[(*E*)-2-(phenyl)-1-diazenyl]quinolin-8-olate.

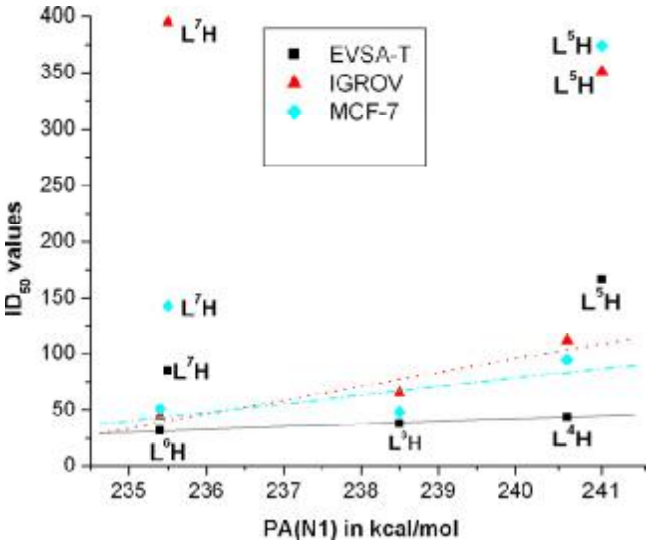

Fig. 8. The correlation between ID_{50} values and the proton affinity (PA) of the N(1) atom of the ligands.

($L^{3-7}H$). The ID_{50} values given in Table 4 show that the activity of the $^nBu_2Sn(L^{3-7})_2$ compounds (**3–7**) decrease in the order **3** < **4** < **5** (Me, OMe and OEt substituents in L^3H, L^4H and L^5H, respectively), whereas the ID_{50} value for **6** (Cl-substituted compound) for all cell lines is higher than that of **3**, the ID_{50} value for **7** (Br-substituted compound) is found to be less than that of **3** for EVSA-T, IGROV and MCF-7 cell lines and slightly higher for other cell lines.

In general, the activity seems to depend upon the basicity of the donor atoms of the ligand employed [62]. The compounds become less active as the basicity increases and this correlation is depicted in Fig. 8. Compounds **5** and **7** with –OEt and –Br substituents (L^5H and L^7H) deviate from the correlation possibly due the solubility problem in DMSO (see Section 2.6 for details). It can be anticipated from this trend that the incorporation of electron withdrawing substituent (such as CF_3) in the ligand of di-*n*-butyltin(IV) compound will possibly enhance the cytotoxic activity. Thus, the test results of the di-*n*-butyltin(IV) compounds (**3–7**) led to important structure-activity information and related work in this area is in progress.

Acknowledgements

The financial support of the Department of Science and Technology, New Delhi, India (Grant Nos. SR/S1/IC-03/2005, TSBB; SR/S1/PC-13/2005, AKC), the University Grants Commission, New Delhi, India through SAP-DSA, Phase-III), the Ministry of Education, Youth and Sports of the Czech Republic (Grant project No. MSM0021627502, RJ and MH) and National Institutes of Health Minority Biomedical Research Support Program, USA (Grant No. GM08005, GE) are gratefully acknowledged. The *in vitro* cytotoxicity experiments were carried out by Ms P.F. van Cuijk in the Laboratory of Translational Pharmacology, Department of Medical Oncology, Erasmus Medical Center, Rotterdam, The Netherlands, under the supervision of Dr. E.A.C. Wiemer and Prof. Dr. G. Stoter.

Appendix A. Supplementary material

CCDC-668200 to CCDC-668203 contain the supplementary crystallographic data for complexes **3–5** and **7**, respectively. These data can be obtained free of charge from The Cambridge Crystallographic Data Centre via http://www.ccdc.cam.ac.uk/data_request/cif. Supplementary data associated with this article can be found, in the online version, at doi:10.1016/j.jinorgbio.2008.05.001.

References

[1] M. Gielen, R. Willem, J. Holeček, A. Lyčka, Main Group Met. Chem. 16 (1993) 29–43.
[2] M. Gielen, E.R.T. Tiekink (Eds.), Metallotherapeutic Drug and Metal-based Diagnostic Agents: The Use of Metals in Medicine, John Wiley & Sons Ltd., Chichester, UK, 2005, pp. 421–430. and references therein.
[3] A. Lyčka, J. Holeček, B. Schneider, J. Straka, J. Organomet. Chem. 389 (1990) 29–39.
[4] A. Lyčka, J. Holeček, A. Sebald, I. Tkac, J. Organomet. Chem. 409 (1991) 331–339.
[5] E.O. Schlemper, Inorg. Chem. 6 (1967) 2012–2017.
[6] W. Chen, W.K. Ng, V.G. Kumar Das, G.B. Jameson, R.J. Butcher, Acta Crystallogr. Sect. C 45 (1989) 861–864.
[7] E. Kellö, V. Vrábel, J. Holeček, J. Sivy, J. Organomet. Chem. 493 (1995) 13–16.
[8] A. Szorcsik, L. Nagy, M. Scopelliti, A. Deák, L. Pellerito, K. Hegetschweiler, J. Organomet. Chem. 690 (2005) 2243–2253.
[9] A. Linden, T.S. Basu Baul, A. Mizar, Acta Crystallogr. Sect. E 61 (2005) m27–m29.
[10] S.W. Ng, C. Wei, V.G. Kumar Das, J.P. Charland, F.E. Smith, J. Organomet. Chem. 364 (1989) 343–351.
[11] M. Schumann, R. Schmiedgen, F. Huber, A. Silvestri, G. Ruisi, A.B. Paulsen, R. Barbieri, J. Organomet. Chem. 584 (1999) 103–117.
[12] T.S. Basu Baul, A. Mizar, X. Song, G. Eng, R. Willem, M. Biesemans, I. Verbruggen, R. Butcher, J. Organomet. Chem. 691 (2006) 2605–2613.
[13] T.S. Basu Baul, A. Mizar, A. Lyčka, E. Rivarola, R. Jirásko, M. Holčapek, D. de Vos, U. Englert, J. Organomet. Chem. 691 (2006) 3416–3425.
[14] J. Ensling, P. Gutlich, K.M. Hassellbach, B.W. Fitzsimmons, J. Chem. Soc. (A) (1971) 1940–1943.
[15] R.C. Poller, J.N.R. Ruddick, J. Organomet. Chem. 39 (1972) 121–128.
[16] T.S. Basu Baul, A. Mizar, E. Rivarola, U. Englert, J. Organomet. Chem. 693 (2008) 1751–1758.
[17] V.L. Narayanan, M. Nasr, K.D. Paul, in: M. Gielen (Ed.), Tin-based Antitumor Drugs, Springer-Verlag, Berlin, 1990, pp. 201–217.
[18] A.J. Crowe, in: M. Gielen (Ed.), Metal Based Antitumour Drugs, vol. 1, Freund, London, 1988, pp. 103–149.
[19] M. Gielen, P. Lelieveld, D. de Vos, R. Willem, in: M. Gielen (Ed.), Metal Based Antitumour Drugs, vol. 2, Freund, Tel Aviv, 1992, pp. 29–54.
[20] C. Pellerito, P.D. Agati, T. Fiore, C. Mansueto, V. Mansueto, G. Stocco, L. Nagy, L. Pellerito, J. Inorg. Biochem. 99 (2005) 1294–1305.
[21] F. Cima, L. Ballarin, Appl. Organomet. Chem. 13 (1999) 697–703.
[22] M.N. Shuaibu, H. Kanbara, T. Yanagi, A. Ichinose, D.A. Ameh, J.J. Bonire, A.J. Nok, Jpn. Parasitolog. Res. 91 (2003) 5–11.
[23] C.E. Carraher Jr., A. Battin, K.R. Shahi, M.R. Roner, J. Inorg. Organomet. Polym. 17 (2007) 631–639.
[24] G. Barot, K.R. Shahi, M.R. Roner, C.E. Carraher, J. Inorg. Organomet. Polym. 17 (2007) 595–603.
[25] M. Roner, C. Carraher, J. Roehr, K. Bassett, J. Polym. Mater. 23 (2006) 153–159.

[26] C. Carraher, D. Siegmann-Louda, Macromolecules Containing Metal and Metal-like Elements, vol. 3, Wiley, Hoboken, NJ, 2004.
[27] P.J. Blower, Inorganic pharmaceuticals, Annu. Rep. Prog. Chem. Sect A 100 (2004) 633–658.
[28] M. Kemmer, M. Gielen, M. Biesemans, D. de Vos, R. Willem, Metal-Based Drugs 5 (1998) 189–196.
[29] M. Kemmer, L. Ghys, M. Gielen, M. Biesemans, E.R.T. Tiekink, R. Willem, J. Organomet. Chem. 582 (1999) 195–203.
[30] M. Gielen, P. Lelieveld, D. de Vos, H. Pan, R. Willem, M. Biesemans, H.H. Fiebig, Inorg. Chim. Acta 196 (1992) 115–117.
[31] M. Bouâlam, M. Gielen, A. El Khloufi, D. de Vos, R. Willem, Novel Organo-tin Compounds having Anti-tumour Activity and Anti-tumour compositions, Pharmachemie B.V., Eur. Pat., Publ 538 517, Appl. 91/202, 746.3-, 22.10.91; Chem. Abstr. 119 (1993) 117548b.
[32] M. Gielen, R. Willem, H. Dalil, D. de Vos, C.M. Kuiper, G.J. Peters, Metal-Based Drugs 5 (1998) 83–90.
[33] A. Růžička, L. Dostál, R. Jambor, V. Buchta, J. Brus, I. Císařová, M. Holčapek, J. Holeček, Appl. Organomet. Chem. 16 (2002) 315–322.
[34] A. Růžička, A. Lyčka, R. Jambor, P. Novák, I. Císařová, M. Holčapek, M. Erben, J. Holeček, Appl. Organomet. Chem. 17 (2003) 168–174.
[35] R. Hooft, KappaCCD Collect Software, Nonius BV, Delft, The Netherlands, 1999.
[36] Z. Otwinowski, W. Minor, in: C.W. Carter Jr., R.M. Sweet (Eds.), Methods in Enzymology, vol. 276, Macromolecular Crystallography, Part A, Academic Press, New York, 1997, pp. 307–326.
[37] R.H. Blessing, Acta Crystallogr. Sect. A 51 (1995) 33–38.
[38] G.M. Sheldrick, SHELXS97, Program for the Solution of Crystal Structures, University of Göttingen, Germany, 1997.
[39] A. Altomare, G. Cascarano, C. Giacovazzo, A. Guagliardi, M.C. Burla, G. Polidori, M. Camalli, SIR92, J. Appl. Crystallogr. 27 (1994) 435.
[40] P. van der Sluis, A.L. Spek, Acta Crystallogr. Sect. A 46 (1990) 194–201.
[41] A.L. Spek, PLATON, Program for the Analysis of Molecular Geometry, University of Utrecht, The Netherlands, 2005.
[42] G.M. Sheldrick, SHELXL97, Program for the Refinement of Crystal Structures, University of Göttingen, Germany, 1997.
[43] M.R. Boyd, Principl. Practice Oncol. 3 (1989) 1–12.
[44] Y.P. Keepers, P.E. Pizao, G.J. Peters, J. Van Ark-Otte, B. Winograd, H.M. Pinedo, Eur. J. Cancer 27 (1991) 897–900.
[45] C. Lee, W. Yang, R.G. Parr, Phys. Rev. 37B (1988) 785–789.
[46] A.K. Chandra, D. Michalska, R. Wysokinsky, T. Zeegers-Huyskens, J. Phys. Chem. Sect. A 108 (2004) 9593–9600.
[47] A.K. Chandra, T. Zeegers-Huyskens, J. Org. Chem. 68 (2003) 3618–3625.
[48] M.J. Frisch et al., Gaussian 03, Revision D.01, Gaussian, Inc., Wallingford, CT, 2004.
[49] C. Hansch, A. Leo, R.W. Taft, Chem. Rev. 91 (1991) 165–195.
[50] L. Pauling, The Nature of Chemical Bond, third ed., Cornell University Press, New York, 1960.
[51] J. Otera, J. Organomet. Chem. 221 (1981) 57–61.
[52] K. Kawasaki, R. Okawara, J. Organomet. Chem. 6 (1966) 249–258.
[53] J. Holeček, M. Nádvorník, K. Handlíř, A. Lyčka, J. Organomet. Chem. 315 (1986) 299–308.
[54] D. Shi, S. Hu, Chin. J. Struct. Chem. 7 (1988) 111.
[55] F. Huber, R. Kaiser, J. Organomet. Chem. 6 (1966) 126–132.
[56] A. Lyčka, J. Holeček, M. Nádvorník, Main Group Met. Chem. 12 (1989) 169–186.
[57] V.K. Jain, J. Mason, B.S. Saraswat, R.C. Mehrotra, Polyhedron 4 (1985) 2089–2096.
[58] R.V. Parish, in: L.S. Kothari, J.S. Baijal, S.P. Tewari (Eds.), Mössabauer Effect: Current Applications to Physical Sciences, Academic Publications, Delhi, India, 1984, p. 162.
[59] R. Barbieri, F. Huber, L. Pellerito, G. Ruisi, A. Silvestri, in: P.J. Smith (Ed.), ^{119}Sn Mössbauer Studies on Tin Compounds, Blackie, London, 1998, pp. 496–540.
[60] R.C. Poller, J.N.R. Ruddick, J. Chem. Soc. (A) (1969) 2273–2276.
[61] L. Kolářová, M. Holčapek, R. Jambor, L. Dostál, A. Růžička, M. Nádvorník, J. Mass Spectrom. 39 (2004) 621–629.
[62] H. Li, C.S. Lai, J. Wu, P.C. Ho, D. De Vos, E.R.T. Tiekink, J. Inorg. Biochem. 101 (2007) 809–816.